Interpretation of specularly reflected optical radiation for determining physical parameters of plates

O.V. Shefer

Tomsk State University
Institute of Atmospheric Optics,
Siberian Branch of the Russian Academy of Sciences, Tomsk

Received May 23, 2002

A numerical model of a polydisperse ensemble of oriented plates is presented within the method of physical optics as applied to bistatic polarization laser sensing of crystal clouds. Characteristics of reflected radiation are investigated numerically as functions of the physical properties of crystals for different wavelengths of incident radiation. The possibility of estimating crystal size and orientation is studied.

Introduction

At present, the much attention is given, in the research community, to the studies of crystal clouds. The problem of radiation transfer in cirrus clouds is among most important investigations. It is known that crystal clouds largely consist of oriented particles.[1] The most stable position in space is characteristic of elongated crystals. As a rule, the state of incident radiation polarization changes at its interaction with oriented particles. The radiation that is being reflected from the crystal sides can cause different optical phenomena in the atmosphere.[2,3] Lidar methods for sounding are widely used for investigation of physical and dynamical parameters of crystal clouds. They enable one to detect not only the intensity of return signal, but also its polarization properties. The latter characteristics of the received radiation bear information on the shape, size, refractive index, and orientation of the cloud particles under study.

Numerical models of crystals are obtained to date for the cases of both chaotic and dominating orientation.[1,4,5] As a rule, these models enable one to estimate the intensity and polarization characteristics as applied to monostatic sounding at wavelengths in the visible range, where the absorption by ice is inessential.

Remote sounding of cirrus clouds by means of a bistatic polarization lidar promises great potentialities. Researchers note prospects of this method as compared with traditional monostatic one.[6] However, no theoretical investigations of angular distributions of the intensity of scattered radiation together with its polarization properties have been carried out until so far as applied to the bistatic sounding. To estimate the experimental data, one uses numerical results obtained for the monostatic sounding.

The numerical model of an individual oriented plate was obtained[7] in the frameworks of physical optics as applied to the bistatic polarization laser sounding of crystal clouds. The choice of this model for investigation of the optical characteristics of atmospheric ice formation was also presented there. The calculated results on polarization characteristics and scattering cross section at the change of the physical parameters of particle were presented in Refs. 8 and 9. The peculiarities revealed in scattering enabled us to select the subject for further investigations in passing to the integral characteristics. In sounding crystal clouds with a bistatic lidar, one can detect maximum possible intensity of the reflected signal in addition to the specific polarization characteristics characteristic of a certain type of particles. Crystals of the plate shape provide for the most intensive reflection. The recorded signal with "anomalously" high amplitude can be used for estimation of the parameters of microstructure. Polarization characteristics of such a signal provides for the more information about the refractive index, the greater is the incline angle of the lidar axis to the plane of dominating orientation of plates.

This paper is the continuation of Refs. 7–9. The results of numerical investigation of the light scattering characteristics of polydisperse medium at different parameters of particle size distribution in the optical wavelength range are presented.

Statement of the problem

Let us investigate the characteristics of electromagnetic field reflected from an ensemble of oriented plates. Let us relate the positions of source, receiver, and the plane of preferred orientation of crystals to the absolute coordinate system by means of the corresponding pair of angles (φ_i, θ_i) $(i = 1, 2, 3)$ of the spherical coordinate system. Let us note that the bistatic sounding scheme used in the numerical experiment has been described in Ref. 7. Obviously, to simulate the case of "strictly specular reflection," one should take into account that the angle between the direction of sounding and the direction normal to the plate base and the angle between the direction toward

0235-6880/02/10 804-06 $02.00 © 2002 Institute of Atmospheric Optics

the receiver and the same normal should be equal to each other. A particle of the simulated medium is characterized by the complex refractive index $\tilde{n} = n + i\chi$ (χ is the absorption coefficient), the radius a, and the thickness d. According to the law of crystallographic growth, the following dependence between the diameter and the thickness of the plate is valid[10]: $d = 2.020\,(2a)^{0.449}$. This relationship significantly simplifies the numerical calculations when passing from a separate crystal to an ensemble of particles.

It was revealed in numerous field investigations of crystal clouds at different temperature regimes that the crystal size distribution has a well-pronounced maximum.[11] The gamma-distribution adequately describes the size spectrum of crystal aerosol:

$$N(a) = N\,\frac{\mu^{\mu+1}}{\Gamma(\mu+1)}\,\frac{1}{a_{\mathrm{m}}}\left(\frac{a}{a_{\mathrm{m}}}\right)^{\mu} \mathrm{e}^{-\mu a/a_{\mathrm{m}}}. \qquad (1)$$

Formula (1) contains the following parameters: N is the number density of plates, a_{m} is the plate radius corresponding to the maximum of function $N(a)$; μ is the dimensionless parameter characterizing the steep slope of this maximum. To analyze the experimental data, it is necessary to transform formula (1) so that the mean plate radius $\overline{a}$ is involved in it. The formula for $\overline{a}$, in the case of gamma-distribution, has the form

$$\overline{a} = a_{\mathrm{m}}\,(1 + 1/\mu). \qquad (2)$$

The relationships for the cross sections of light scattering to the backward hemisphere (we call backward hemisphere the part of the sphere which is limited by the plate base and contains the incident and reflected beams) were obtained in Ref. 7 in the frameworks of the method of physical optics. The model presented enables one to calculate the light scattering characteristics at any point of the hemisphere for both polarized and unpolarized incident radiation at arbitrary positions of the source, particle, and receiver. Then, the formulas for the scattering cross sections σ_{π_i} ($i = 1, 2, 3, 4$) obtained in Ref. 7 have the form

$$\begin{aligned}
\sigma_{\pi_1} &= W\left\{M_{11} + \frac{I_2}{I_1}M_{12} + \frac{I_3}{I_1}M_{13} + \frac{I_4}{I_1}M_{14}\right\},\\
\sigma_{\pi_2} &= W\left\{M_{21} + \frac{I_2}{I_1}M_{22} + \frac{I_3}{I_1}M_{23} + \frac{I_4}{I_1}M_{24}\right\}, \qquad (3)\\
\sigma_{\pi_3} &= W\left\{M_{31} + \frac{I_2}{I_1}M_{32} + \frac{I_3}{I_1}M_{33} + \frac{I_4}{I_1}M_{34}\right\},\\
\sigma_{\pi_4} &= W\left\{M_{41} + \frac{I_2}{I_1}M_{42} + \frac{I_3}{I_1}M_{43} + \frac{I_4}{I_1}M_{44}\right\}.
\end{aligned}$$

The factor W is determined by the wave number and the angular function, which is the Fraunhofer integral; I_i ($i = 1, 2, 3, 4$) are the Stokes parameters of the incident radiation; M_{ij} are the elements of the scattering phase matrix ($i = 1, 2, 3, 4$; $j = 1, 2, 3, 4$).

To study the light scattering characteristics of a polydisperse medium, let us consider the integral representation of the scattering coefficients

$$\beta_{\pi_i} = \int N(a)\,\sigma_{\pi_i}\,\mathrm{d}a \quad (i = 1, 2, 3, 4), \qquad (4)$$

where $N(a)$ is the particle size distribution function.

Let us pay the principal attention in this paper to the study of the dependence of the first scattering coefficient β_{π_1} which is proportional to the intensity I_{π_1} of signal coming to the receiver, and to the polarization characteristics. The transmitter which transform the linearly polarized radiation or the radiation with circular polarization is more often used in laser sounding of the atmosphere. Analyzing the polarization properties of scattered radiation, let us consider in a more detail the ratio of the scattering coefficients β_{π_i} ($i = 1, 2$) proportional to the corresponding Stokes parameters I_{π_i} ($i = 1, 2$) in the case of a linearly polarized incident radiation

$$P_2 = \frac{I_{\pi_2}}{I_{\pi_1}} = \frac{\beta_{\pi_2}}{\beta_{\pi_1}}. \qquad (5)$$

Scattered radiation is partially polarized at interaction of the unpolarized radiation with oriented crystals. To study the spectral dependence of the degree of polarization St at different physical parameters, let us use the following formula:

$$St = (I_{\pi_2}^2 + I_{\pi_3}^2 + I_{\pi_4}^2)^{1/2} \,/\, I_{\pi_1}. \qquad (6)$$

Thus, the purposes of this paper are the following:

– to study the light scattering characteristics determined by formulas (4)–(6) and reveal their dependences on the physical parameters of the medium and the wavelength of incident radiation;

– to study the "fine structure" of the dependence of the amplitude of the reflected signal at angular scanning with the receiver;

– to estimate the possibility of determining the physical parameters of the medium tested on the basis of analysis of the presented data.

Discussion of numerical results

For qualitative analysis of radiation specularly reflected from oriented particles with flat sides researchers use such a parameter as reflectivity. It is known that the reflectivity of ice at the incidence angles β from 60 to 90° sharply increases up to almost 100%. To calculate the energy characteristic in the wave zone, one takes into account the cross section of the beam in the direction perpendicular to the direction of radiation propagation.[12]

For calculating the quantitative characteristics of light scattering, let us use the formulas (4) for the scattering coefficients. These formulas relate the

polarization and energy properties of the reflected radiation to the physical parameters of the polydisperse medium (size spectrum of semi-transparent particles), to the wavelength, and to the state of polarization of the incident radiation at the corresponding positions of a source, receiver, and the plane of preferred orientation of plates.

Table 1 presents the values of scattering coefficient β_{π_1} proportional to the intensity of specularly reflected radiation for some realistic parameters of the particle size distribution $\bar{a}$, N, and μ of natural crystal clouds. The "anomalously" high values of the scattering coefficient well explain the fact that the photodetectors broke down in the majority of events when recording the specularly reflected light.[13] One can visually observe bright columns in the atmosphere, which are formed by reflection of light from the plane sides of oriented crystals.[2] The scattering coefficient β_{π_1} linearly depends on the number density of crystals N (see formulas (1) and (4)). Analyzing the data presented in Table 1 and applying interpolation, if necessary, one can estimate the values of the scattering coefficient at any number density of particles with different mean size and the distribution parameter μ. It is seen from Table 1 that, as $\bar{a}$ increases by tens of micrometers, the amplitude of the specularly reflected signal changes by orders of magnitude.

The values of the scattering cross sections proportional to the first parameter of the Stokes vector were presented in Refs. 8 and 9. It was shown that, in spite of the existence of the regular dependence of the scattering cross section σ_{π_1} on particle orientation relative to the source and the receiver, the values of the extreme points of the curve σ_{π_1} are determined by the combination of angles (φ_1, θ_1), (φ_2, θ_2), (φ_3, θ_3). Theoretical investigation of the "effect of anomalous backscatter" was carried out in Ref. 14 as applied to the monostatic scheme of lidar sounding. The values of the coefficient of the specular reflection of radiation for the same parameters of the medium N, $\bar{a}$, and μ that were used for calculating the values presented in Table 1 were presented here. For example, for $\beta = 0°$, $\bar{a} = 37$ μm, $N = 0.8$ l^{-1}, $\mu = 5$ the value $\beta_{\pi_1} = 16.2$ km^{-1}. The experimentally measured backscattering coefficient[13] for the same parameters was $\beta_{\pi_1} = 17$ km^{-1}. By comparing numerical and experimental values, it is easy to draw certain conclusions not only on their qualitative, but also on the quantitative coincidence. The calculated and presented in Table 1 values of the coefficient of specular reflection of radiation for $\beta = 20°$ at the corresponding parameters of the medium is equal to 11.6 km^{-1}. In this case the enhanced value $\beta_{\pi_1} = 16.2$ km^{-1} at $\beta = 0°$, as compared with $\beta_{\pi_1} = 11.6$ km^{-1} at $\beta = 20°$ is explained by the fact that, although the reflectivity is approximately the same at this angle (it differs by some percent), the cross section of the specularly reflected beam decreases as β increases.

The characteristic evidence of the case of specular reflection is a sharp decrease of the amplitude of recorded signal when scanning with a receiver from the direction corresponding to the "strictly specular reflection." It follows from the analysis of the numerical data presented in Table 2, that even an insignificant displacement of the angle ϑ (ϑ is the angle between the lines of receiving and the specular reflection) of the direction of receiving leads to a noticeable variation in the scattering coefficient β_{π_1}.

Table 1. Calculated values of the specular reflection coefficient β_{π_1} (km^{-1}) of an ensemble of oriented plates for linearly polarized incident radiation [complex refractive index $\tilde{n} = 1.31 + i\cdot 10^{-3}$, wavelength $\lambda = 0.694$ μm), $\theta_1 = -40°$, $\theta_2 = 100°$, $\theta_3 = -60°$, $\beta = 20°$, $\varphi_i = 0°$ ($i = 1, 2, 3$)]

μ	$\bar{a}$, μm				
	37	100	150	200	250
	N, l^{-1}				
	0.8	25	20	15	10
1	0.37416E+02	0.62388E+05	0.25267E+06	0.59883E+06	0.97244E+06
2	0.22172E+02	0.36971E+05	0.14973E+06	0.35492E+06	0.57765E+06
3	0.16370E+02	0.27295E+05	0.11054E+06	0.26203E+06	0.42648E+06
4	0.13410E+02	0.22360E+05	0.90557E+05	0.21465E+06	0.34937E+06
5	0.11641E+02	0.19410E+05	0.78609E+05	0.18633E+06	0.30328E+06
6	0.10472E+02	0.17461E+05	0.70719E+05	0.16763E+06	0.27283E+06
7	0.96463E+01	0.16084E+05	0.65142E+05	0.15441E+06	0.25132E+06
8	0.90332E+01	0.15062E+05	0.61002E+05	0.14460E+06	0.23535E+06
9	0.85608E+01	0.14274E+05	0.57811E+05	0.13703E+06	0.22304E+06
10	0.81860E+01	0.13649E+05	0.55280E+05	0.13103E+06	0.21327E+06
11	0.78816E+01	0.13142E+05	0.53225E+05	0.12616E+06	0.20534E+06

Note: the number 0.37416E+02 and analogous designate the value $0.37416\cdot 10^2$.

Table 2. Calculated values of the specular reflection coefficient β_{π_1} (km^{-1}) of the system of oriented plates at circular polarization of the incident radiation [complex refractive index $\tilde{n} = 1.31 + i\cdot10^{-3}$, $\mu = 5$, $\theta_1 = -40°$, $\theta_2 = 100°$, $\varphi_i = 0°$ ($i = 1, 2, 3$)]

$\theta_3°$	$\vartheta°$	$\bar{a}$, μm				
		37	100	150	200	250
		N, l^{-1}				
		0.8	25	20	15	10
λ = 0.694 μm						
−60.0	0.0	0.11640E+02	0.19409E+05	0.78608E+05	0.18633E+06	0.30327E+06
−59.99	0.01	0.11538E+02	0.18159E+05	0.67715E+05	0.14329E+06	0.20227E+06
−59.98	0.02	0.11228E+02	0.14931E+05	0.44300E+05	0.70070E+05	0.71252E+05
−59.95	0.05	0.93029E+01	0.45629E+04	0.52473E+04	0.43231E+04	0.33160E+04
−59.9	0.1	0.49936E+01	0.45062E+03	0.48965E+03	0.48967E+03	0.40781E+03
−59.8	0.2	0.81722E+00	0.51092E+02	0.61182E+02	0.61052E+02	0.50821E+02
−59.5	0.5	0.38893E−01	0.32685E+01	0.39178E+01	0.39178E+01	0.32630E+01
−59.0	1.0	0.48835E−02	0.41119E+00	0.49329E+00	0.49324E+00	0.41102E+00
−58.0	2.0	0.61794E−03	0.52150E−01	0.62576E−01	0.62574E−01	0.52145E−01
−55.0	5.0	0.41044E−04	0.34661E−02	0.41593E−02	0.41593E−02	0.34661E−02
λ = 10.6 μm						
−60.0	0.0	0.49897E−01	0.83199E+02	0.33696E+03	0.79871E+03	0.13000E+04
−59.9	0.1	0.49878E−01	0.81123E+02	0.31698E+03	0.71488E+03	0.10921E+04
−59.95	0.5	0.46012E−01	0.42876E+02	0.83534E+02	0.86226E+02	0.63315E+02
−59.0	1.0	0.35099E−01	0.90443E+01	0.84414E+01	0.76533E+01	0.63176E+01
−55.0	5.0	0.64309E−03	0.53171E−01	0.63655E−01	0.63599E−01	0.52978E−01
−50.0	10.0	0.82429E−04	0.69227E−02	0.83021E−02	0.83003E−02	0.69162E−02
−40.0	20.0	0.10585E−04	0.89228E−03	0.10706E−02	0.10706E−02	0.89205E−03
−30.0	30.0	0.30198E−05	0.25477E−03	0.30569E−03	0.30569E−03	0.25473E−03

Note. The numbers 0.37416E+02, 0.38893E−01, and analogous designate the values $0.37416\cdot10^2$ and $0.38893\cdot10^{-1}$.

Then, at bistatic sounding, using radiation with the wavelength λ = 0.694 μm, of a cloud containing the oriented plates the deviation of the axis of receiving from the direction of the specular reflection by only 1° leads to a decrease of the amplitude of the recorded signal by 4–7 orders of magnitude. Such a change in the IR wavelength range (λ = 10.6 μm) is 1–3 orders of magnitude. The decrease of the amplitude by 4–7 orders of magnitude (at λ = 10.6 μm) corresponds to the scanning angle of 20–30°. One should note that the steep slope of the characteristic β_{π_1} in the range of small angles ϑ is unambiguously related to the mean size $\bar{a}$ of the plate crystals. This makes it possible to estimate the mean size of the spatially oriented crystals from the relative change of the amplitude of the recorded signal at scanning with a lidar (or with the receiver) near the direction realizing the case of "strictly specular reflection."

The coefficient of specular reflection of radiation is non-linearly related to the wavelength and the parameters of the particle size distribution $\bar{a}$ and μ. The increase of $\bar{a}$ and μ leads to an increase in the amplitude of the reflected signal, while it decreases as λ increases. It is seen from Tables 1 and 2 that the rates of the change of $\beta_{\pi 1}$ as function of $\bar{a}$, μ, and λ are different.

The study of interaction of visible and IR radiation with aerosol media is of specific interest in the problems on propagation of optical radiation through the atmosphere. Let us study some characteristics of light scattering in the wavelength range from 0.5 to 15 μm. It was mentioned above that as the angle between the direction of the incidence of radiation and the direction normal to the base of the plate particle increases, the reflectivity increases. When determining the energy characteristics of light scattering in the wave zone, one should take into account the cross section of the specularly reflected beam, the area of which becomes greater, with the increasing angle β. Hence, the wavelength behavior of the light scattering curves in combination with different angular characteristics is not evident.

To calculate the spectral behavior of light scattering characteristics, let us use the dependences $n = n(\lambda)$ and $\chi = \chi(\lambda)$ constructed using the data from Ref.11 and shown in Fig. 1.

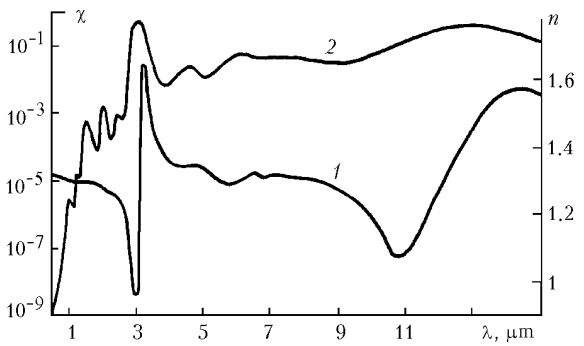

Fig. 1. Real and imaginary parts of the complex refractive index of ice as functions of wavelength: $n(\lambda)$ (curve *1*); $\chi(\lambda)$ (curve *2*).

The spectral dependences of the coefficient of specular reflection of radiation at changing positions of particles relative to the sounding path are shown in Fig. 2. The angle β is equal to 20, 35, and 40° for the curves *1–3* (Fig. 2), respectively. The maximum difference in the values $\beta_{\pi 1}$ for different sounding paths is observed at azimuth angles $\varphi_i = 0°$ (i = 1, 2, 3). The difference between the curves disappears at the change of one of the angles (for example, at $\varphi_1 \to 90°$).

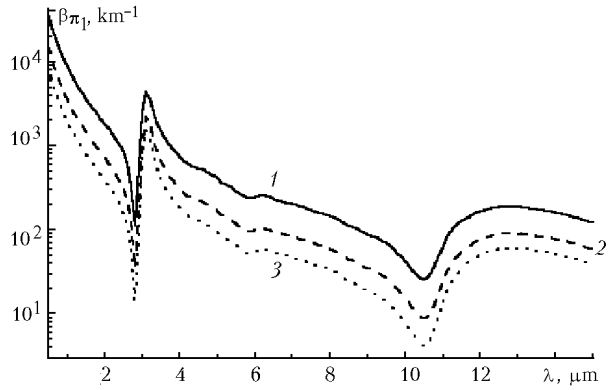

Fig. 2. The dependence of the coefficient of specular reflection $\beta_{\pi 1}(\lambda)$ at linearly polarized incident radiation ($I_2/I_1 = 1$, $I_4 = I_3 = 0$); $\bar{a}$ = 125 μm, N = 10 l^{-1}, μ = 5, $\varphi_1 = 0°$, $\varphi_2 = 0°$, $\theta_2 = 100°$: $\theta_1 = -40°$, $\theta_3 = -60°$ (*1*); $\theta_1 = -10°$, $\theta_3 = -45°$ (*2*); $\theta_1 = 0°$, $\theta_3 = -40°$ (*3*).

It is seen from Fig. 2 that the spectral dependence of $\beta_{\pi_1}(\lambda)$ is similar in part to the behavior of the curve $n(\lambda)$ for ice (see Fig. 1), showing all principal maxima and minima. However, the behavior of the curves in the visible and near IR wavelength ranges (see Fig. 2) significantly differs from almost invariable $n(\lambda)$ behavior (see Fig. 1). In this range we observe the change of the values β_{π_1} by some orders of magnitude.

Spectral dependences of the ratio of the scattering coefficients $P_2 = \beta_{\pi_2}/\beta_{\pi_1}$ in the case of linearly polarized incident radiation at different angles φ_1 and θ_1 are shown in Fig. 3. Let us note that the neutral behavior of $P_2(\lambda)$ is observed at $\varphi_1 = 0°$, and the spectral dependence is observed at $\varphi_1 \neq 0°$, and it is better pronounced at larger values of the azimuth angle φ_1. The exceptions are the cases of $\varphi_1 = 90$ and 180°. The coordinates of the extreme points $P_2(\lambda)$ correspond to the positions of the minima and maxima of $n(\lambda)$ (see Fig. 1).

It is seen from comparison of the values of the spectral dependences $P_2(\lambda)$ at the same θ_1 but different φ_1 (curves *1* and *3*) that P_2 is most sensitive to the changes of λ at large β. The positions of the minimum and maximum of P_2 are unambiguously related to the azimuth angle, which determines the orientation of the reference plane.

The dependences of the degree of polarization St on λ are shown in Fig. 4*a*. The strongest variations of the spectral dependence $St(\lambda)$ are observed in the wavelength range from 10 to 12 μm, and are equal to approximately 3 μm. Its peculiarities are unambiguously related to the angles of radiation incidence. The less is the value of β the less is the degree of polarization. As was shown in our paper,[9] the degree of polarization is greater for larger φ_1 value, all other factors being the same. This peculiarity is confirmed by the dependences *1* and *3* in Fig. 4*a*. Analyzing the presented dependences $St(\lambda)$, one can conclude that the unpolarized radiation becomes almost completely polarized at specular reflection from plates at large inclination angles of the sounding path relative to the direction normal to the plane of orientation of the plates.

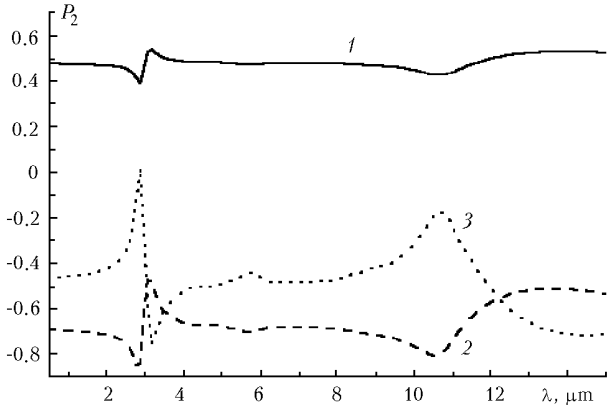

Fig. 3. The dependence of $P_2(\lambda)$ at linearly polarized incident radiation ($I_2/I_1 = 1$, $I_4 = I_3 = 0$), $\varphi_2 = 0°$, $\theta_2 = 100°$: $\theta_1 = -40°$, $\varphi_1 = 40°$, β = 26° (*1*); $\theta_1 = 0°$, $\varphi_1 = 40°$, β = 40° (*2*); $\theta_1 = -40°$, $\varphi_1 = 140°$, β = 55° (*3*).

Radiation becomes partially linearly polarized at specular reflection of light from oriented plates. The spectral dependence of the ratio $P_2(\lambda)$ calculated for the same parameters as $St(\lambda)$ (Fig. 4*a*) is shown in Fig. 4*b*. Comparing the corresponding curves in Figs. 4*a* and *b*, one can see that the positions of the extreme points of the curves $St(\lambda)$ and $P_2(\lambda)$ coincide. At the same time, the positions of the minima of $St(\lambda)$ correspond to the positions of the maxima in $P_2(\lambda)$, and the positions of the maxima in $St(\lambda)$ correspond to the positions of the minima in $P_2(\lambda)$.

In studying the propagation of light in the atmosphere, it is necessary to take into account the possibility and the character of the ability of oriented crystals to polarize incident radiation as a function of not only the positions of the source and the particles, but also of the wavelength of incident radiation.

This paper presents a number of light scattering characteristics at specular reflection from plates without taking into account the flatter. However, crystals under natural conditions oscillate about their stable position. Obviously, such deviations lead to the decrease of the amplitude of the reflected signal. The numerical investigation of the specularly reflected radiation from crystals taking into account their possible flatter will be presented in our next papers.

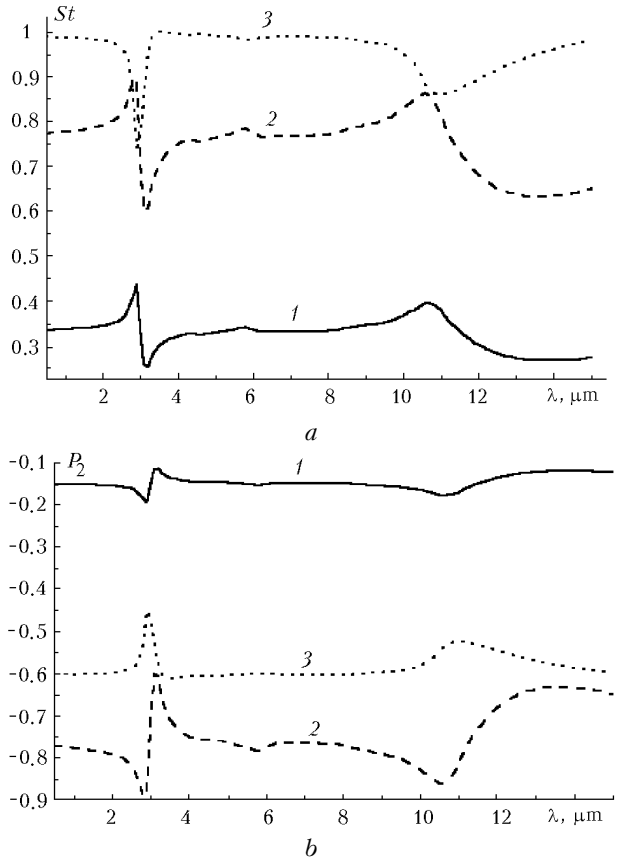

Fig. 4. The dependence of the degree of polarization $St(\lambda)$ (*a*) and the ratio $P_2(\lambda)$ (*b*) for the unpolarized incident radiation ($I_1 = 1$, $I_2 = I_4 = I_3 = 0$); $\bar{a} = 125$ μm, $\lambda = 10.6$ μm, $\varphi_2 = 0°$, $\theta_2 = 100°$: $\theta_1 = -40°$, $\varphi_1 = 40°$, $\beta = 26°$ (*1*); $\theta_1 = 0°$, $\varphi_1 = 40°$, $\beta = 40°$ (*2*); $\theta_1 = -40°$, $\varphi_1 = 140°$, $\beta = 55°$ (*3*).

Conclusion

The necessary condition of the formation of reflected radiation with "anomalously" high amplitude is the presence of oriented ice plates in the cloud. The relationship is obtained for the coefficient of the specularly reflection of optical radiation from an ensemble of such crystals, which enables us to estimate the reflected signal and to relate it to the physical parameters of a polydisperse medium and the characteristics of incident radiation.

It has been revealed from numerical analysis of the scattering coefficient, that the intensity of the recorded signal decreases by 1–7 orders of magnitude at displacement of the direction of receiving from the line of the "strictly specular reflection" by only 1°. It is shown that one can determine the mean size of the plates from the estimate of the coefficient of the specular reflection of radiation even in cirrus clouds of a complex composition. Analysis of the polarization characteristics, in particular, the ratio of the parameters of the Stokes vector and the degree of polarization has shown the possibility of determining the spatial position of the system of oriented plates. The spectral behavior of the scattering coefficient and polarization characteristics in the visible and IR range is determined by the physical parameters of particles and their position with respect to the source and the receiver, as well as by the state of polarization of incident radiation. The peculiarities of these dependences illustrate the possibility of unambiguously determining the microphysical parameters of the crystals from the data of multi-frequency sounding.

Acknowledgments

The work was supported in part by Russian Foundation for Basic Research (Grant No. 01–05–65209), Ministry of Industry, Science and Technology of Russian Federation (Grant "High-Altitude Polarization Lidar," No. 06–21).

References

1. M.I. Mischenko, J.W. Hovenier, and L.D. Travis, eds., *Light Scattering by Nonspherical Particles. Theory, Measurements, and Application* (Academic Press, California, USA, 2000), 690 pp.
2. A. Mallman, J.L. Hock, and R.G. Greenler, Appl. Opt. **37**, 1441–1449 (1998).
3. K. Sassen, J. Optics & Photonics News, No. 3, 39–42 (1999).
4. D.N. Romashov, Atmos. Oceanic Opt. **14**, No. 2, 102–110 (2001).
5. A. Borovoi, I. Grishin, and U. Oppel, Opt. Lett. **25**, No. 18, 388–390 (2000).
6. B.M. Welsh and Ch.S. Gardner, Appl. Opt. **28**, No. 1, 32–82 (1989).
7. O.V. Shefer, Atmos. Oceanic Opt. **12**, No. 7, 549–553 (1999).
8. O.V. Shefer, Atmos. Oceanic Opt. **12**, No. 12, 1029–1036 (1999).
9. O.V. Shefer, Atmos. Oceanic Opt. **14**, No. 8, 607–612 (2001).
10. A. Auer and D. Veal, J. Atmos. Sci. **27**, No. 6, 919–926 (1970).
11. O.A. Volkovitskii, L.N. Pavlova, and A.G. Petrushin, *Optical Properties of Crystal Clouds* (Gidrometeoizdat, Leningrad, 1984), 200 pp.
12. K. Sassen, J. Opt. Soc. Amer. A. **4**, No. 3, 570–580 (1987).
13. C.M.R. Platt, J. Appl. Meteorol. **17**, No. 4, 482–488 (1978).
14. A.A. Popov and O.V. Shefer, Appl. Opt. **33**, No. 30, 7038–7044 (1994).